Adjoint analysis of Buckley-Leverett and two-phase flow equations

Computational Geosciences manuscript No.
(will be inserted by the editor)

Adjoint Analysis of Buckley-Leverett and Two-phase Flow Equations

Savithru Jayasinghe · David L. Darmofal · Marshall C. Galbraith · Nicholas K. Burgess · Steven R. Allmaras

Received: date / Accepted: date

Abstract This paper analyzes the adjoint equations and boundary conditions for porous media flow models, specifically the Buckley-Leverett equation, and the compressible two-phase flow equations in mass conservation form. An adjoint analysis of a general scalar hyperbolic conservation law whose primal solutions include a shock jump is initially presented, and the results are later specialized to the Buckley-Leverett equation. The non-convexity of the Buckley-Leverett flux function results in adjoint characteristics that are parallel to the shock front upstream of the shock, and emerge from the shock front downstream of the shock. Thus, in contrast to the behavior of Burgers' equation where the adjoint is continuous at a shock, the Buckley-Leverett adjoint, in general, contains a discontinuous jump across the shock. Discrete adjoint solutions from space-time discontinuous Galerkin finite element approximations of the Buckley-Leverett equation are shown to be consistent with the derived closed-form analytical solutions. Furthermore, a general result relating the adjoint equations for different (though equivalent) primal equations is used to relate the compressible two-phase flow adjoints to the Buckley-Leverett adjoint. Adjoint solutions from space-time discontinuous Galerkin finite element approximations of the two-phase flow equations are observed to obey this relationship.

Keywords adjoint solutions · Buckley-Leverett · two-phase flow · conservation law · continuous analysis · shockwaves

This research was supported through a Research Agreement with Saudi Aramco, a Founding Member of the MIT Energy Initiative (http://mitei.mit.edu/), with technical monitors Dr. Ali Dogru and Dr. Nicholas Burgess.

S. Jayasinghe · D. Darmofal · M. Galbraith · S. Allmaras
Massachusetts Institute of Technology,
77 Massachusetts Ave., Cambridge, MA
E-mail: savithru@mit.edu, darmofal@mit.edu, galbramc@mit.edu, allmaras@mit.edu

N. Burgess
Aramco Services Company,
400 Technology Square, Cambridge, MA
E-mail: nburgess3@gmail.com

Nomenclature

u	Scalar primal solution
f	1D spatial flux
x_s	Spatial location of shock
$\dot{x}_s$	Speed of shock
$\vec{F}$	Space-time flux
Ω	Space-time domain
Γ_s	Path of shock in space-time
J	Output functional
ψ, ψ_s	Scalar adjoint solutions
ϕ	Porosity
S_w, S	Wetting-phase saturation
u_T	Total velocity
f_w	Wetting-phase fractional flow function
μ_w, μ_n	Wetting and non-wetting phase viscosities
p	Wetting phase pressure
p_c	Capillary pressure
ρ_w, ρ_n	Wetting and non-wetting phase densities
λ_w, λ_n	Wetting and non-wetting phase mobilities
q_w, q_n	Wetting and non-wetting phase sources
K	Rock permeability
ψ_w, ψ_n	Wetting and non-wetting phase adjoint solutions

1 Introduction

The adjoint equations to a set of partial differential equations (the primal equations) are useful for computing the sensitivity of an objective function to perturbations in the primal problem. For optimization of PDE-constrained problems, adjoint analysis is an efficient approach to determine the sensitivity of a problem when the number of objective functions and constraints is much smaller than the number of design parameters (controls) [15,24]. For porous media flows, which are the focus of this paper, an important application of adjoint analysis is data assimilation (or history-matching) in which the initial conditions, boundary conditions, and model parameters are adjusted so that the flow solution best matches the available measured data. The optimized primal problem can then be used as the basis of a predictive model for future behavior. Adjoint-based sensitivity analysis methods have been used for performing history matching in single-phase [8,7,29,26], multi-phase [30,24,18,2] and compositional flow problems [9,23].

Adjoint solutions also play an important role in the analysis and control of numerical errors. Becker and Rannacher have developed the dual-weighted residual (DWR) method based on the fundamental result that the residual of the approximate primal solution weighted by the adjoint is the error in the objective function [5,6]. With this insight, Becker and Rannacher developed a grid adaptive method to control a DWR-based estimate of this objective function error. While the DWR method fits most naturally with finite element discretizations, the key ideas have been extended to other discretizations [12,17,4]. An extensive literature now exists on a variety of DWR-based adaptive methods applied to a wide range of problems [27,28,20,31,10,25,22,21].

Most applications of the adjoint method outlined above make use of a discrete adjoint solution that is obtained by linearizing the discrete residual operator. Although the discrete adjoint method works for general problems, it does not necessarily provide a clear insight into the nature of the adjoint solution. An analytic approach can be used to provide a theoretical understanding of the adjoint PDE, boundary conditions, and solution behavior, which can then also be used to verify discrete adjoint solutions on simplified problems.

This work is motivated by the desire for a theoretical understanding of the adjoint equations for representative models of porous media flows. Specifically, the focus is on the Buckley-Leverett equation and a two-equation two-phase flow model. First, the adjoint equation for a general nonlinear scalar hyperbolic conservation law is derived, and then the result is specialized to the Buckley-Leverett equation. While adjoint analyses for nonlinear scalar hyperbolic equations have been performed previously [13,11], the specific case of the Buckley-Leverett equation has not been considered. In particular, the non-convexity of the Buckley-Leverett flux function, which gives rise to entropy-satisfying solutions with combined rarefaction-shock waves, results in an adjoint solution that does not require a boundary condition at the shock for the region upstream of the shock. This is in contrast to the adjoint behavior of equations with convex fluxes, such as Burgers' equation, where the adjoint is continuous across a shock [1].

Further, numerical adjoint solutions obtained using the space-time discontinuous Galerkin (DG) finite element method detailed in [22] are shown to be consistent with the closed-form analytic solutions of the Buckley-Leverett adjoint equation derived in this work. The numerical method employs an *adjoint consistent* formulation [19], which ensures that the discrete adjoint problem is a consistent discretization of the continuous adjoint problem. It is expected that any adjoint consistent discrete numerical scheme, independent of the use of a space-time approach or a finite-element method, will produce discrete adjoint solutions that are consistent with the analytic ones presented in this paper. Hence, these analytic solutions can serve as reference data to validate the implementations of such numerical schemes.

Finally, this paper presents a derivation of the analytic adjoint equations for the compressible two-phase flow equations in mass conservation form, which is a generalization of the Buckley-Leverett equation. Furthermore, the adjoint solutions of the two-phase flow problem are shown to be directly related to the adjoint solution of the Buckley-Leverett equation.

2 Scalar conservation laws with shocks

This section presents a derivation of two 1D scalar conservation law adjoint equations with different output functional types. These general results are later specialized to the case of the Buckley-Leverett equation and compared against numerical results. Consider the 1D scalar conservation law given in Eq. (1), with the initial and boundary conditions given by Eq. (2) - (3).

$$\frac{\partial u}{\partial t} + \frac{\partial f}{\partial x} = 0, \tag{1}$$

$$u(x,0) = u_0(x), \qquad x \in [0, L] \tag{2}$$

$$u(0,t) = u_L(t), \qquad t \in [0, T] \tag{3}$$

Without loss of generality, characteristics are assumed to enter the domain from the left boundary at all times

($\frac{\partial f}{\partial u} > 0$ at $x = 0$). If the solution $u(x,t)$ contains shocks, then the Rankine-Hugoniot jump condition,

$$\dot{x}_s \left[\!\left[u\right]\!\right] - \left[\!\left[f\right]\!\right] = 0, \tag{4}$$

must be satisfied, where $x_s(t)$ and $\dot{x}_s$ represent the spatial location and speed of the shock respectively. The jump operator in 1D, defined as $\left[\!\left[\cdot\right]\!\right] = (\cdot)^+ - (\cdot)^-$, represents the jump in a certain quantity between the left $(+)$ and right $(-)$ sides of the shock. The primal problem described by Eq. (1) - (4) is represented in the following space-time form:

$$\nabla \cdot \vec{F} = 0, \qquad \vec{x} \in \Omega, \tag{5}$$

where $\vec{x} = (x,t)$ is the augmented space-time coordinate, $\Omega = [0,L] \times [0,T]$ is the space-time domain, and $\vec{F}$ represents the space-time fluxes,

$$\vec{F} = (F_x(u), F_t(u)) = (f(u), u)\,. \tag{6}$$

The Rankine-Hugoniot jump condition given in Eq. (4) transforms to the equivalent jump condition in space-time, given by:

$$\left[\!\left[-\vec{F}\right]\!\right] = 0, \qquad \vec{x} \in \Gamma_s, \tag{7}$$

where Γ_s is the curve that tracks the path of the shock, and the jump operator definition has been extended to multiple dimensions for scalar and vector quantities as follows,

$$\left[\!\left[s\right]\!\right] = s^+\vec{n}^+ + s^-\vec{n}^- = (s^+ - s^-)\vec{n}^+, \tag{8}$$

$$\left[\!\left[\vec{v}\right]\!\right] = \vec{v}^+ \cdot \vec{n}^+ + \vec{v}^- \cdot \vec{n}^- = (\vec{v}^+ - \vec{v}^-) \cdot \vec{n}^+, \tag{9}$$

where $\vec{n}^+$ is the space-time unit normal vector pointing from the left to the right of interface Γ_s, and $\vec{n}^- = -\vec{n}^+$. The components of the space-time unit normal vector $\vec{n}^+ = \left(n_x^+, n_t^+\right)$ depend on the shock speed as follows:

$$n_x^+ = \frac{1}{\sqrt{\dot{x}_s^2 + 1}}, \qquad n_t^+ = \frac{-\dot{x}_s}{\sqrt{\dot{x}_s^2 + 1}}. \tag{10}$$

A schematic of the space-time domain and the shock path is given in Figure 1.

Let Ω_1 and Ω_2 be partitions of the space-time domain to the left and right of the shock respectively, separated by the interface Γ_s as shown in Figure 1. The boundaries of Ω_1 and Ω_2, including Γ_s, are denoted by Γ_1 and Γ_2 respectively. Next, consider the weak form of the primal equations in $\Omega_1 \cup \Omega_2$ and the Rankine-Hugoniot relation across Γ_s:

$$R(u, x_s, w, w_s) = \int_{\Omega_1 \cup \Omega_2} w \nabla \cdot \vec{F} d\Omega - \int_{\Gamma_s} w_s \left[\!\left[\vec{F}\right]\!\right] d\Gamma, \tag{11}$$

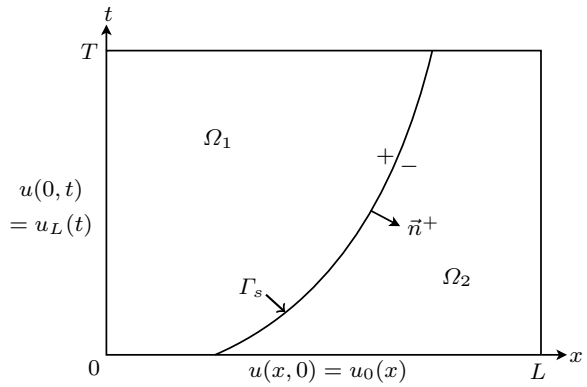

Fig. 1 Schematic of space-time domain Ω

where w and w_s are admissible test functions. The linearized form of Eq. (11) is obtained by considering infinitesimal perturbations of the solution, denoted by $\delta u(x,t)$, and the shock location, denoted by $\delta x_s(t)$. Perturbing the shock location by $\delta x_s(t)$ results in a horizontal perturbation of the shock interface Γ_s by a vector $\vec{\delta}_s = (\delta x_s(t), 0)$. The resulting perturbed weak form is given by Eq. (12).

$$\begin{aligned} R + \delta R = &\int_{\Omega_1 \cup \Omega_2} w \nabla \cdot (\vec{F} + \delta\vec{F}) d\Omega \\ &+ \int_{\Gamma_s} w^+ (\nabla \cdot \vec{F}^+) \vec{\delta}_s \cdot \vec{n}^+ d\Gamma \\ &- \int_{\Gamma_s} w^- (\nabla \cdot \vec{F}^-) \vec{\delta}_s \cdot \vec{n}^+ d\Gamma \\ &- \int_{\Gamma_s} w_s \left[\!\left[(\vec{F} + \delta\vec{F})\right]\!\right] d\Gamma \\ &- \int_{\Gamma_s} w_s \left(\vec{F}^+ - \vec{F}^-\right) \cdot \delta\vec{n}^+ \, d\Gamma \end{aligned} \tag{12}$$

Using the definition of R in Eq. (11) to cancel out terms, and rewriting in terms of the jump operator yields:

$$\begin{aligned} \delta R = &\int_{\Omega_1 \cup \Omega_2} w \nabla \cdot (\delta\vec{F}) d\Omega + \int_{\Gamma_s} \left[\!\left[w(\nabla \cdot \vec{F})\right]\!\right] \cdot \vec{\delta}_s \, d\Gamma \\ &- \int_{\Gamma_s} w_s \left[\!\left[\delta\vec{F}\right]\!\right] d\Gamma - \int_{\Gamma_s} w_s \left(\vec{F}^+ - \vec{F}^-\right) \cdot \delta\vec{n}^+ \, d\Gamma. \end{aligned} \tag{13}$$

Note that the second integral in Eq. (13) vanishes since $\nabla \cdot \vec{F} = 0$. Invoking the chain rule to represent the flux

perturbations $\delta\vec{F}$ in terms of δu and δx_s gives:

$$\begin{aligned}\delta R = &\int_{\Omega_1\cup\Omega_2} w\nabla\cdot\left(\vec{A}\delta u\right)d\Omega \\ &-\int_{\Gamma_s} w_s\left[\!\!\left[\left(\vec{A}\delta u\right)+\frac{\partial\vec{F}}{\partial x}\delta x_s\right]\!\!\right]d\Gamma \\ &-\int_{\Gamma_s} w_s\left(\vec{F}^+-\vec{F}^-\right)\cdot\delta\vec{n}^+\,d\Gamma,\end{aligned} \tag{14}$$

where $\vec{A}=\frac{\partial\vec{F}}{\partial u}$. Performing integration by parts on the volume integral yields:

$$\begin{aligned}\delta R = &-\int_{\Omega_1\cup\Omega_2}\nabla w\cdot\left(\vec{A}\delta u\right)d\Omega \\ &+\int_{\Gamma_1\cup\Gamma_2} w\left(\vec{A}\delta u\right)\cdot\vec{n}\,d\Gamma \\ &-\int_{\Gamma_s} w_s\left[\!\!\left[\left(\vec{A}\delta u\right)+\frac{\partial\vec{F}}{\partial x}\delta x_s\right]\!\!\right]d\Gamma \\ &-\int_{\Gamma_s} w_s\left(\vec{F}^+-\vec{F}^-\right)\cdot\delta\vec{n}^+\,d\Gamma.\end{aligned} \tag{15}$$

The boundary integral in Eq. (15) is separated into an integral over the shock interface Γ_s and an integral over the domain boundary, $\Gamma_B = (\Gamma_1\cup\Gamma_2)\backslash\Gamma_s$, as shown below:

$$\begin{aligned}\delta R = &-\int_{\Omega_1\cup\Omega_2}\nabla w\cdot\left(\vec{A}\delta u\right)d\Omega+\int_{\Gamma_B} w\left(\vec{A}\delta u\right)\cdot\vec{n}\,d\Gamma \\ &+\int_{\Gamma_s}\left(\left[\!\!\left[w\left(\vec{A}\delta u\right)\right]\!\!\right]-w_s\left[\!\!\left[\left(\vec{A}\delta u\right)\right]\!\!\right]\right)d\Gamma \\ &-\int_{\Gamma_s} w_s\left(\left[\!\!\left[\frac{\partial\vec{F}}{\partial x}\delta x_s\right]\!\!\right]+\left(\vec{F}^+-\vec{F}^-\right)\cdot\delta\vec{n}^+\right)d\Gamma.\end{aligned} \tag{16}$$

The expression inside the brackets in the last integral of Eq. (16) is simplified using the approach outlined in Appendix A, resulting in the following equation for δR:

$$\begin{aligned}\delta R(\delta u,\delta x_s,w,w_s) = &\\ &-\int_{\Omega_1\cup\Omega_2}\nabla w\cdot\left(\vec{A}\delta u\right)d\Omega \\ &+\int_{\Gamma_B} w\left(\vec{A}\delta u\right)\cdot\vec{n}\,d\Gamma \\ &+\int_{\Gamma_s}\left(\left[\!\!\left[w\left(\vec{A}\delta u\right)\right]\!\!\right]-w_s\left[\!\!\left[\left(\vec{A}\delta u\right)\right]\!\!\right]\right)d\Gamma \\ &+\int_{\Gamma_s} w_s\frac{d}{dt}\left((F_t^+-F_t^-)\delta x_s\right)n_x^+ d\Gamma.\end{aligned} \tag{17}$$

Given a generic output functional $J(u)$ and its linearization $\delta J(\delta u,\delta x_s)$, the adjoint solutions ψ and ψ_s satisfy the following equation for all $\delta u,\delta x_s$ [14]:

$$\delta R(\delta u,\delta x_s,\psi,\psi_s)=\delta J(\delta u,\delta x_s). \tag{18}$$

The relationship of these adjoint solutions to the calculation of output sensitivities, as required for inverse analysis and design optimization, is described in Appendix B.

The following sub-sections formulate the adjoint equation and boundary conditions for two different output functionals.

2.1 Output: spatial integral at $t = T$

This section assumes that the output functional of interest is the spatial integral of some solution dependent quantity $g(u)$ at $t = T$:

$$J_T=\int_0^L g(u(x,T))dx. \tag{19}$$

Splitting the output into integrals to the left and right of the shock and linearizing gives:

$$\begin{aligned}\delta J_T(\delta u,\delta x_s) = &\int_0^{x_s(T)}\frac{\partial g}{\partial u}\delta u(x,T)\,dx \\ &+\int_{x_s(T)}^{L}\frac{\partial g}{\partial u}\delta u(x,T)\,dx+[\![g]\!]_{t=T}\,\delta x_s(T),\end{aligned} \tag{20}$$

where $[\![g]\!]_{t=T}$ represents the jump in the value of g across the shock at the final time T.

The adjoint definition (Eq. (18)) with this output yields:

$$\begin{aligned}&-\int_{\Omega_1\cup\Omega_2}\nabla\psi\cdot\left(\vec{A}\delta u\right)d\Omega+\int_{\Gamma_B}\psi\left(\vec{A}\delta u\right)\cdot\vec{n}\,d\Gamma \\ &+\int_{\Gamma_s}\left(\left[\!\!\left[\psi\left(\vec{A}\delta u\right)\right]\!\!\right]-\psi_s\left[\!\!\left[\left(\vec{A}\delta u\right)\right]\!\!\right]\right)d\Gamma \\ &+\int_{\Gamma_s}\psi_s\frac{d}{dt}\left((F_t^+-F_t^-)\delta x_s\right)n_x^+ d\Gamma \\ &=\int_0^{x_s(T)}\frac{\partial g}{\partial u}\delta u(x,T)\,dx+\int_{x_s(T)}^{L}\frac{\partial g}{\partial u}\delta u(x,T)\,dx \\ &\quad+[\![g]\!]_{t=T}\,\delta x_s(T).\end{aligned} \tag{21}$$

The adjoint PDE is obtained by equating volume integrals on both sides of Eq. (21) and noting that the resulting equation is valid for any perturbation δu.

$$-\int_{\Omega_1\cup\Omega_2}\nabla\psi\cdot\left(\vec{A}\delta u\right)d\Omega=0 \tag{22}$$

$$\boxed{\nabla\psi\cdot\frac{\partial\vec{F}}{\partial u}=0} \tag{23}$$

The adjoint boundary conditions are obtained by collecting the domain boundary integrals in Eq. (21). All domain boundary integrals at $t = 0$ and $x = 0$ vanish since the primal initial condition and left boundary condition requires $\delta u(x, 0)$ and $\delta(0, t)$ to be zero, respectively. As a result, there are no adjoint boundary conditions at the bottom ($t = 0$) and left ($x = 0$) boundaries. The absence of a primal boundary condition at the right ($x = L$) boundary implies that $\delta u(L, t) \neq 0$, hence requiring the following adjoint boundary condition in order for the boundary integrals at $x = L$ to vanish:

$$\boxed{\psi(L, t) = 0.} \tag{24}$$

The boundary integrals at $t = T$ give:

$$\begin{aligned} &\int_0^{x_s(T)} \psi(x,T)\frac{\partial F_t}{\partial u}\delta u(x,T)\ dx \\ &+ \int_{x_s(T)}^{L} \psi(x,T)\frac{\partial F_t}{\partial u}\delta u(x,T)\ dx \\ &= \int_0^{x_s(T)} \frac{\partial g}{\partial u}\delta u(x,T)\ dx + \int_{x_s(T)}^{L} \frac{\partial g}{\partial u}\delta u(x,T)\ dx. \end{aligned} \tag{25}$$

Requiring Eq. (25) to hold for any perturbation $\delta u(x, T)$ yields the following adjoint boundary condition at $t = T$:

$$\boxed{\psi(x,T)\frac{\partial F_t}{\partial u}(x,T) = \frac{\partial g}{\partial u}(x,T), \qquad \forall x \neq x_s(T).} \tag{26}$$

The behavior of the adjoint variables at the shock is found by analyzing the shock interface integrals in Eq. (21). Collecting all shock interface integrals that depend on δx_s gives:

$$\int_{\Gamma_s} \psi_s \frac{d}{dt}\left((F_t^+ - F_t^-)\delta x_s\right) n_x^+ d\Gamma = [\![g]\!]_{t=T}\, \delta x_s(T). \tag{27}$$

Performing integration by parts in time using $d\Gamma = dt/n_x^+$, and noting that $\delta x_s(0) = 0$ due to the primal initial condition, yields:

$$\begin{aligned} &\psi_s(T)\,[\![F_t]\!]_{t=T}\,\delta x_s(T) \\ &- \int_0^T \frac{d\psi_s}{dt}(F_t^+ - F_t^-)\delta x_s dt = [\![g]\!]_{t=T}\,\delta x_s(T), \end{aligned} \tag{28}$$

where $[\![F_t]\!]_{t=T}$ is the jump in F_t across the shock at time T. Requiring Eq. (28) to hold for any $\delta x_s(t)$ gives the following conditions for $\psi_s(t)$:

$$\psi_s(T)\,[\![F_t]\!]_{t=T} = [\![g]\!]_{t=T}\,, \tag{29}$$

$$\frac{d\psi_s}{dt} = 0. \tag{30}$$

Therefore, ψ_s is a constant which takes the following value:

$$\boxed{\psi_s = \frac{[\![g]\!]_{t=T}}{[\![F_t]\!]_{t=T}}.} \tag{31}$$

Lastly, the third integral on the left-hand side of Eq. (21) gives the following condition across the shock:

$$\left[\!\left[\psi\left(\vec{A}\delta u\right)\right]\!\right] = \psi_s \left[\!\left[\left(\vec{A}\delta u\right)\right]\!\right]. \tag{32}$$

Expanding all components of Eq. (32) using the definitions of $\vec{A}$ and Eq. (101) yields:

$$\begin{aligned} &\left(\psi^+ - \psi_s\right)\left(\frac{\partial F_x}{\partial u}^+ - \dot{x}_s\frac{\partial F_t}{\partial u}^+\right)\delta u^+ \\ &-\left(\psi^- - \psi_s\right)\left(\frac{\partial F_x}{\partial u}^- - \dot{x}_s\frac{\partial F_t}{\partial u}^-\right)\delta u^- = 0. \end{aligned} \tag{33}$$

Conditions on ψ^+, ψ^- and ψ_s are obtained by analyzing the nature of the terms in Eq. (33). If $\left(\frac{\partial F_x}{\partial u}^+ - \dot{x}_s\frac{\partial F_t}{\partial u}^+\right)$ is non-zero, then $\psi^+ = \psi_s$ satisfies Eq. (33) for any variation δu^+. By the same argument, $\psi^- = \psi_s$, if $\left(\frac{\partial F_x}{\partial u}^- - \dot{x}_s\frac{\partial F_t}{\partial u}^-\right)$ is non-zero. This is the case for the Burgers' equation, where the adjoint is continuous across the shock (i.e. $\psi^+ = \psi_s = \psi^-$) [1].

However, if $\left(\frac{\partial F_x}{\partial u}^+ - \dot{x}_s\frac{\partial F_t}{\partial u}^+\right)$ or $\left(\frac{\partial F_x}{\partial u}^- - \dot{x}_s\frac{\partial F_t}{\partial u}^-\right)$ is identically zero for a particular set of primal fluxes, then the equality of ψ^+ and ψ_s, or ψ^- and ψ_s respectively, cannot be inferred from Eq. (33) alone. In particular, the Buckley-Leverett equation contains this complexity, and Section 3 gives a more detailed analysis of Eq. (33) in this context.

2.2 Output: volume integral over space-time domain

This section assumes that the output functional of interest is the integral of some solution dependent quantity $g(u)$ over the entire space-time domain:

$$J = \int_\Omega g(u) d\Omega. \tag{34}$$

The linearized output variation is given by:

$$\delta J(\delta u, \delta x_s) = \int_{\Omega_1 \cup \Omega_2} \frac{\partial g}{\partial u}\delta u\ d\Omega + \int_{\Gamma_s} [\![g]\!] \cdot \vec{\delta}_s d\Gamma. \tag{35}$$

Using the same approach as in Section 2.1, the adjoint definition given by Eq. (18) yields:

$$
\begin{aligned}
&- \int_{\Omega_1 \cup \Omega_2} \nabla\psi \cdot \left(\vec{A}\delta u\right) d\Omega + \int_{\Gamma_B} \psi \left(\vec{A}\delta u\right) \cdot \vec{n}\; d\Gamma \quad (36)\\
&+ \int_{\Gamma_s} \left(\left[\!\left[\psi \left(\vec{A}\delta u\right) \right]\!\right] - \psi_s \left[\!\left[\left(\vec{A}\delta u\right) \right]\!\right] \right)\; d\Gamma \\
&+ \int_{\Gamma_s} \psi_s \frac{d}{dt} \left((F_t^+ - F_t^-)\delta x_s \right) n_x^+ d\Gamma \\
&= \int_{\Omega_1 \cup \Omega_2} \frac{\partial g}{\partial u}\delta u \; d\Omega + \int_{\Gamma_s} [\![g]\!] \cdot \vec{\delta}_s d\Gamma.
\end{aligned}
$$

From this, the adjoint PDE is given by:

$$\boxed{\nabla\psi \cdot \frac{\partial \vec{F}}{\partial u} = -\frac{\partial g}{\partial u}.} \quad (37)$$

The adjoint boundary conditions are determined by following the discussion in Section 2.1. However, the change in output functional gives a different adjoint BC at $t = T$:

$$\boxed{\psi(x, T) = 0, \qquad \forall x \neq x_s(T).} \quad (38)$$

Manipulating the integrals along the shock in Eq. (36) gives the following ODE for $\psi_s(t)$:

$$\boxed{\frac{d\psi_s}{dt} = -\frac{g^+ - g^-}{F_t^+ - F_t^-},} \quad (39)$$

subject to the condition:

$$\boxed{\psi_s(T) = 0.} \quad (40)$$

3 Buckley-Leverett equation

This section applies the results of Section 2 to the case of the Buckley-Leverett problem:

$$\frac{\partial}{\partial t}(\phi S_w) + \frac{\partial}{\partial x}(u_T f_w(S_w)) = 0, \quad (41)$$

$$S_w(x, 0) = 0.1, \quad x \in [0, L] \quad (42)$$

$$S_w(0, t) = 1, \quad t \in [0, T] \quad (43)$$

where the wetting phase saturation S_w is the dependent variable, porosity $\phi = 0.3$, and total velocity $u_T = 0.3$ ft/day. S_w is a non-dimensional quantity that takes physical values in the range $[0, 1]$. The fractional flow function $f_w(S_w)$ [3] is a nonlinear, non-convex function defined as:

$$f_w(S_w) = \frac{S_w^2}{S_w^2 + \frac{\mu_w}{\mu_n}(1 - S_w)^2}. \quad (44)$$

In this work, the wetting-phase to non-wetting phase viscosity ratio $\frac{\mu_w}{\mu_n}$ is assumed to be equal to 0.5, and the relative permeabilities are modeled as quadratic functions. The domain length L is equal to 50 ft, and the final time T is 25 days. The fluxes for this PDE are:

$$\vec{F} = [F_x(S_w), F_t(S_w)] = [u_T f_w(S_w),\ \phi S_w]. \quad (45)$$

The solution to this particular problem is a combined rarefaction-shock wave that originates at $x = 0$. The downstream state of the shock is given by the initial saturation value in the domain:

$$S_w(x_s^-, t) = 0.1. \quad (46)$$

The upstream state of the shock can be obtained by solving the following nonlinear problem, which equates the characteristic speed on the upstream state of the shock to the shock speed given by the Rankine-Hugoniot jump condition:

$$
\begin{aligned}
\frac{u_T}{\phi}\frac{df_w(S_w^+)}{dS_w} &= \frac{u_T}{\phi}\left(\frac{f_w(S_w^+) - f_w(S_w^-)}{S_w^+ - S_w^-}\right) \\
\frac{df_w(S_w^+)}{dS_w} &= \frac{f_w(S_w^+) - f_w(0.1)}{S_w^+ - 0.1}, \quad (47)
\end{aligned}
$$

$$S_w(x_s^+, t) = \frac{\sqrt{249} - 3}{24} \approx 0.53249. \quad (48)$$

The corresponding shock speed is given by:

$$\dot{x}_s(t) = \frac{u_T}{\phi}\frac{\partial f_w}{\partial S_w}^+ = 1.61324 \text{ ft/day}. \quad (49)$$

Figure 2 contains a plot of the primal space-time solution obtained using a second-order discontinuous Galerkin (DG) finite element method, on a structured triangular space-time mesh with 750,000 degrees of freedom (DOF). Figure 3 shows the familiar Buckley-Leverett saturation front propagating to the right at a constant speed, obtained from constant-time slices of the space-time solution in Figure 2. The numerical solutions from the space-time DG method (solid lines) agree well with the analytical solution (dashed lines). This figure clearly shows the compound wave behavior of the Buckley-Leverett solution, where a rarefaction wave is observed upstream (to the left) of the propagating shock.

Figure 4 depicts characteristic paths of the Buckley-Leverett problem defined above. The characteristic paths downstream of the shock either end at the shock (blue region), or leave the domain through the top ($t = T$) and right ($x = L$) boundaries (grey and red regions respectively). Upstream of the shock, all characteristics leave the top boundary. The equality of the limiting upstream characteristic speed and the shock speed (Eq. (49)) causes the limiting upstream characteristic to be parallel to the shock front.

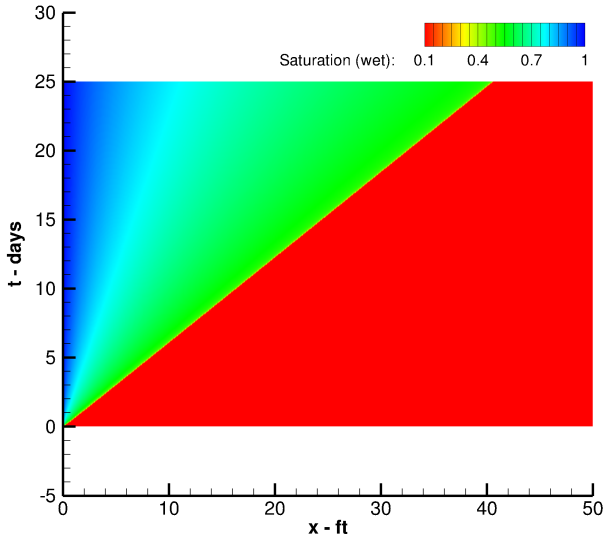

Fig. 2 Primal solution of Buckley-Leverett problem using a second-order space-time DG method with 750,000 DOF.

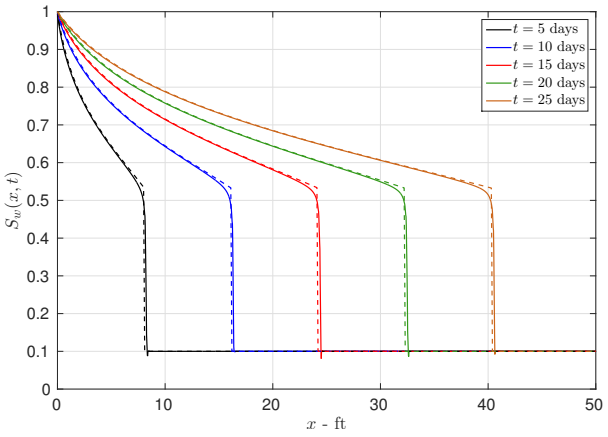

Fig. 3 Comparison of space-time DG (solid lines) and exact (dashed lines) primal solutions at different times.

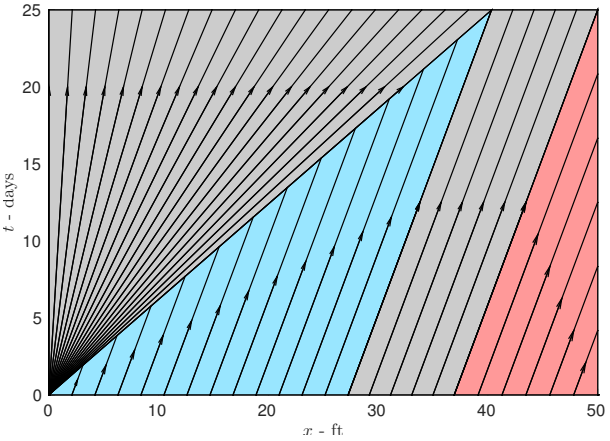

Fig. 4 Primal characteristics of the Buckley-Leverett problem entering the shock (blue region) or exiting the top (grey region) and right (red region) boundaries.

3.1 Output: spatial integral at $t = T$

This section presents the adjoint problem and its solution for the Buckley-Leverett problem defined above, for the output functional given in Eq. (50).

$$J_T = \int_0^L g(S_w(x,T))dx = \int_0^L S_w^2(x,T)dx \tag{50}$$

Using Eq. (23), the adjoint equation for this problem is:

$$\phi\frac{\partial\psi}{\partial t} + \left(u_T\frac{\partial f_w}{\partial S_w}\right)\frac{\partial\psi}{\partial x} = 0. \tag{51}$$

Following the discussion on boundary conditions in Section 2.1, no adjoint boundary conditions are required at the left or bottom boundaries. The boundary conditions at the right and top boundaries follow from Eq. (24) and (26) respectively:

$$\psi(L,t) = 0, \qquad \forall t \in [0,T] \tag{52}$$

$$\psi(x,T) = \frac{2S_w(x,T)}{\phi}, \qquad \forall x \neq x_s(T). \tag{53}$$

The value of ψ_s is computed from Eq. (31):

$$\psi_s = \frac{[\![g]\!]_{t=T}}{[\![\phi S_w]\!]_{t=T}} = \frac{1}{\phi}\left(S_w(x_s^+,T) + S_w(x_s^-,T)\right). \tag{54}$$

The analytical values of S_w on either side of the shock, given previously, reduce Eq. (54) to:

$$\psi_s = \psi(x_s^-,t) = \frac{1}{36}(5\sqrt{249} - 3) \approx 2.10830. \tag{55}$$

Finally, Eq. (33) gives:

$$\begin{aligned}&\left(\psi^+ - \psi_s\right)\left(u_T\frac{\partial f_w}{\partial S_w}^+ - \phi\dot{x}_s\right)\delta u^+ \\ &-\left(\psi^- - \psi_s\right)\left(u_T\frac{\partial f_w}{\partial S_w}^- - \phi\dot{x}_s\right)\delta u^- = 0.\end{aligned} \tag{56}$$

Since the upstream characteristic speed converges to the shock speed (Eq. (49)), the upstream flux term in Eq. (56) vanishes, yielding:

$$\left(\psi(x_s^-,t) - \psi_s\right)\left(u_T\frac{\partial f_w}{\partial S_w}^- - \phi\dot{x}_s\right)\delta u^- = 0. \tag{57}$$

Recognizing that the characteristic speed to the right of the shock does not generally match the shock speed, and requiring Eq. (57) to hold for any δu^- gives the following condition on the adjoint:

$$\psi(x_s^-,t) = \psi_s(t). \tag{58}$$

Eq. (56) cannot give a relationship between $\psi(x_s^+,t)$ and $\psi_s(t)$ because the first term vanishes, which means that these two quantities differ by an arbitrary amount.

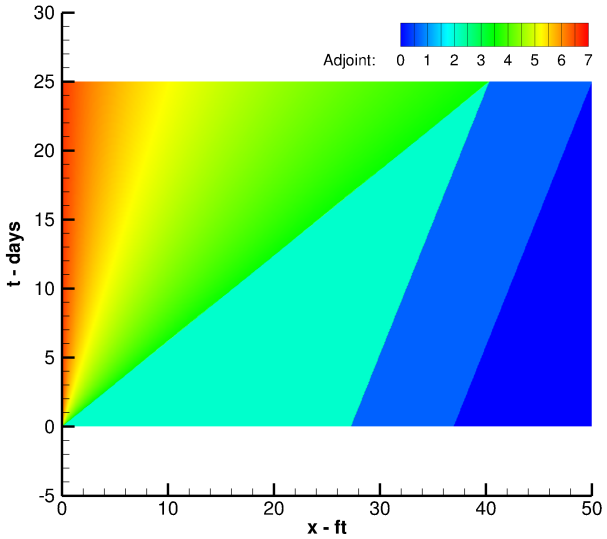

Fig. 5 Exact adjoint solution for output J_T.

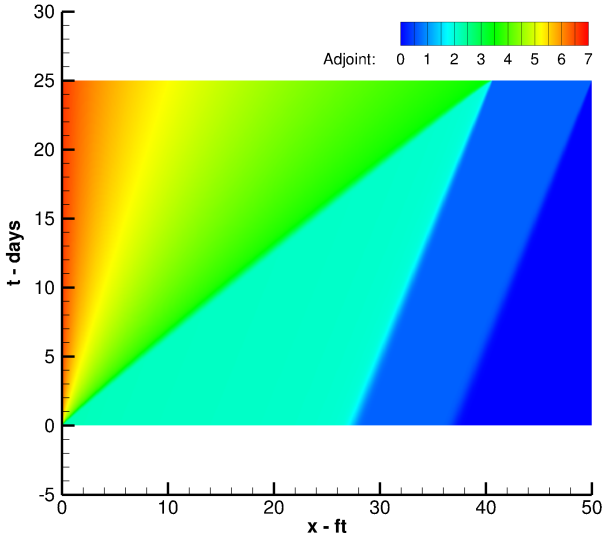

Fig. 6 Numerical adjoint solution for output J_T from a second-order space-time DG method with 750,000 DOF.

However, by using the method of characteristics outlined in Appendix C, the value of $\psi(x_s^+, t)$ is obtained by tracing the characteristic path to the top boundary, where the value of ψ is given by Eq. (53). Note that this result differs from the usual result obtained for PDEs with convex fluxes, such as the Burgers' equation, where characteristics flow into the shock from both sides causing the adjoint variable to be continuous across the shock (i.e. $\psi(x_s^+, t) = \psi(x_s^-, t) = \psi_s(t)$) [16,11]. However, the rarefaction-shock behavior of the Buckley-Leverett equation causes this property to no longer hold, allowing a finite jump between $\psi(x_s^+, t)$ and $\psi_s(t)$.

Figure 5 shows a contour plot of the analytical adjoint solution in the space-time domain, computed by analyzing the characteristics of the adjoint equation in

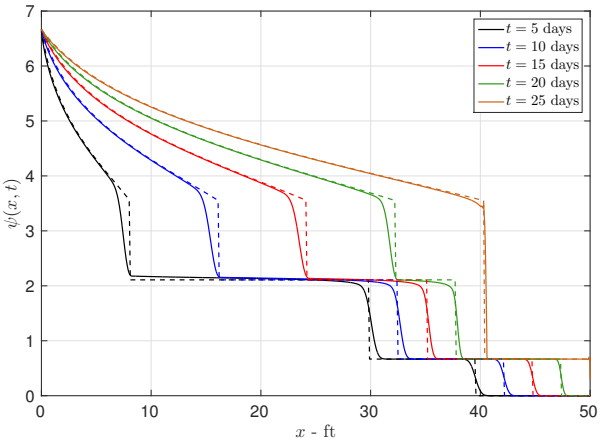

Fig. 7 Comparison of space-time DG (solid lines) and exact (dashed lines) adjoint solutions at different times, for output J_T.

Eq. (51) (as outlined in Appendix C). Figure 6 contains the same plot with a numerical adjoint solution, obtained by a second-order DG finite element method, on a structured triangular mesh with 750,000 degrees of freedom.

The adjoint solution has a constant value of ψ_s along all characteristics emanating from the shock. Furthermore, the absence of a source term in the adjoint PDE (Eq. (51)) means that $\psi(x,t)$ is also constant along each characteristic that emanates from the top and right boundaries. Figure 7 compares the DG adjoint solutions (solid lines) at different times, with the corresponding exact solutions (dashed lines). The numerical results agree well with the analytical solutions, with the largest errors occuring around discontinuities as a result of numerical diffusion.

3.2 Output: volume integral over space-time domain

This section presents the adjoint problem and its solution for the Buckley-Leverett problem, with the output functional given in Eq. (59).

$$J = \int_\Omega g(S_w) d\Omega = \int_\Omega S_w^2(x,t) d\Omega \tag{59}$$

Noting that J is exactly in the form of the general output function considered in Section 2.2, the results derived previously are applicable to this specific problem. Using Eq. (37), the adjoint equation for this problem is given by:

$$\phi \frac{\partial \psi}{\partial t} + \left(u_T \frac{\partial f_w}{\partial S_w} \right) \frac{\partial \psi}{\partial x} = -\frac{\partial g}{\partial S_w}. \tag{60}$$

As before, no adjoint BCs are required for the left and bottom boundaries, and the right boundary remains a

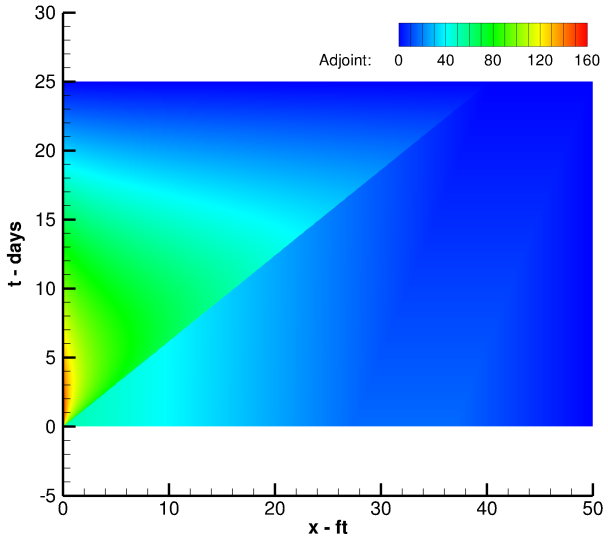

Fig. 8 Exact adjoint solution for output J.

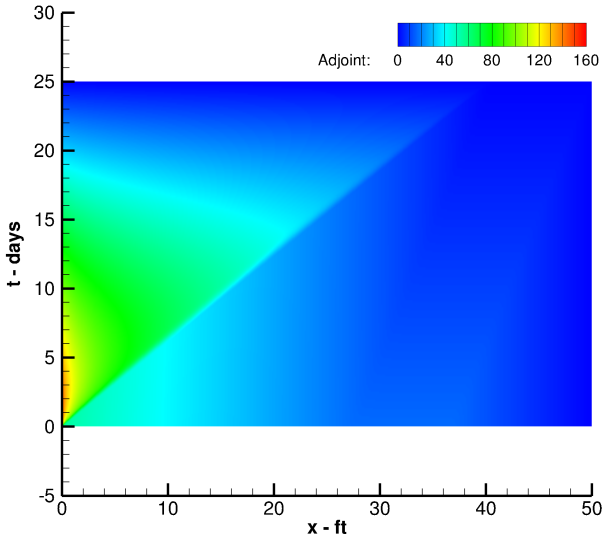

Fig. 9 Numerical adjoint solution for output J from a second-order space-time DG method with 750,000 DOF.

homogeneous Dirichlet condition. The adjoint boundary condition at $t = T$ is exactly as given in Eq. (38):

$$\psi(x, T) = 0, \qquad \forall x \neq x_s(T). \tag{61}$$

The results given in Eq. (56) - (58) are valid for this output functional as well, showing that $\psi(x_s^-, t) = \psi_s(t)$, and that $\psi(x_s^+, t)$ and $\psi_s(t)$ may differ by an arbitrary amount.

The ODE governing $\psi_s(t)$, given by Eq. (39) - (40), simplifies to the following:

$$\frac{d\psi_s}{dt} = -\frac{1}{\phi}\left(S_w(x_s^+, t) + S_w(x_s^-, t)\right), \tag{62}$$

subject to the condition:

$$\psi_s(T) = 0. \tag{63}$$

Noting that the exact solution of S_w to the left and right of the shock is constant in time, and solving the ODE given by Eq. (62) - (63) yields the following expression for $\psi_s(t)$:

$$\psi_s(t) = \frac{1}{\phi}\left(S_w(x_s^+, t) + S_w(x_s^-, t)\right)(T - t) \tag{64}$$

$$= \frac{1}{36}(5\sqrt{249} - 3)(T - t). \tag{65}$$

Figure 8 shows a contour plot of the analytical adjoint solution in the space-time domain, obtained using the approach outlined in Appendix C. Figure 9 contains the same plot for the numerical adjoint solution, obtained by a second-order discontinuous Galerkin finite element method on a structured triangular space-time mesh with $750,000$ degrees of freedom. The source term in Eq. (60) causes the adjoint to increase along each characteristic path emanating from shock, or the top and right boundaries. Figure 10 compares the DG adjoint solutions (solid lines) at different times, with the corresponding exact solutions (dashed lines). The space-time DG solutions agree well with the analytical results in general, except in the vicinity of solution discontinuities.

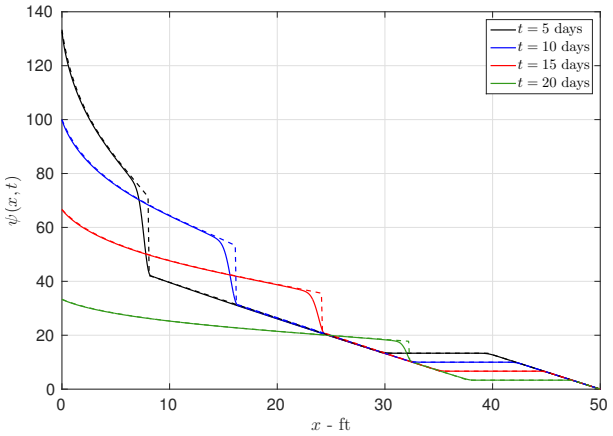

Fig. 10 Comparison of space-time DG (solid lines) and exact (dashed lines) adjoint solutions at different times, for output J.

4 Two-phase flow equations

This section presents a derivation of the adjoint equations for the compressible two-phase flow equations in mass conservation form. The wetting phase pressure $p(x, t)$ and the wetting phase saturation $S(x, t)$ are chosen as the dependent states. The governing equations for the wetting (w) and non-wetting (n) phases are

given by:

$$(\rho_w \phi S)_t \quad - (\rho_w K \lambda_w p_x)_x \quad = \rho_w q_w \tag{66}$$
$$(\rho_n \phi (1-S))_t - (\rho_n K \lambda_n (p_x + p_c' S_x))_x = \rho_n q_n, \tag{67}$$

where $\rho_w(p)$ and $\rho_n(p)$ are the phase densities, $\lambda_w(S)$ and $\lambda_n(S)$ are the phase mobilities, K is the rock permeability, $\phi(p)$ is the rock porosity, $p_c(S)$ is the capillary pressure, and $q_w(p,S)$ and $q_n(p,S)$ are source/sink terms for each phase. All spatial and temporal derivatives are denoted with $(\cdot)_x$ and $(\cdot)_t$ subscripts respectively, while all derivatives with respect to the state variables are denoted with primes (i.e. $\frac{\partial \rho_w}{\partial p} = \rho_w'$ and $\frac{\partial \lambda_w}{\partial S} = \lambda_w'$). Furthermore, $\frac{\partial p_c}{\partial S}$ is replaced with $\gamma(S)$ for the rest of this paper.
Eq. (66) and (67) is written in the space-time formulation as:

$$\nabla \cdot \vec{\mathbf{F}}(\mathbf{u}, \nabla \mathbf{u}) - \mathbf{Q}(\mathbf{u}) = 0, \qquad \vec{x} \in \Omega, \tag{68}$$

where $\mathbf{u} = (p, S)^T$,

$$\vec{\mathbf{F}}(\mathbf{u}, \nabla \mathbf{u}) = \begin{pmatrix} \vec{F}_w \\ \vec{F}_n \end{pmatrix} \tag{69}$$
$$= \left[\begin{pmatrix} -\rho_w K \lambda_w p_x \\ -\rho_n K \lambda_n (p_x + \gamma S_x) \end{pmatrix}, \begin{pmatrix} \rho_w \phi S \\ \rho_n \phi (1-S) \end{pmatrix} \right],$$
$$\mathbf{Q}(\mathbf{u}) = \begin{pmatrix} Q_w \\ Q_n \end{pmatrix} = \begin{pmatrix} \rho_w q_w \\ \rho_n q_n \end{pmatrix}, \tag{70}$$

and $\Omega = [0, L] \times [0, T]$ is the space-time domain as before.

4.1 Output: volume integral over space-time domain

The adjoint analysis of the two-phase flow equations assumes the following volume integrated output functional:

$$J = \int_\Omega g(\mathbf{u}) \, d\Omega. \tag{71}$$

The extension of this analysis to boundary integral outputs follows the procedure described in Section 2.1 for the Buckley-Leverett equation. As before, the adjoint derivation considers infinitesimal perturbations to the solution, $\delta \mathbf{u}$, and equates the linearized weak form to the linearized output:

$$\int_\Omega \boldsymbol{\psi}^T \left(\nabla \cdot \delta \vec{\mathbf{F}} - \delta \mathbf{Q} \right) d\Omega = \int_\Omega \delta g \, d\Omega, \tag{72}$$

where the adjoint vector $\boldsymbol{\psi} = (\psi_w, \psi_n)^T$ contains the adjoint solutions for the wetting and non-wetting phase equations respectively.

Expanding out the terms of each phase equation yields:

$$\int_\Omega \psi_w \left(\nabla \cdot \delta \vec{F}_w - \delta Q_w \right) d\Omega$$
$$+ \int_\Omega \psi_n \left(\nabla \cdot \delta \vec{F}_n - \delta Q_n \right) d\Omega = \int_\Omega \delta g \, d\Omega. \tag{73}$$

Performing integration by parts and substituting in the flux definitions, the integrand of the volume integral is given by:

$$\begin{aligned} &- (\psi_w)_t \, \delta(\rho_w \phi S) \\ &+ (\psi_w)_x \, \delta(\rho_w K \lambda_w p_x) \\ &- (\psi_n)_t \, \delta(\rho_n \phi (1-S)) \\ &+ (\psi_n)_x \, \delta(\rho_n K \lambda_n (p_x + \gamma S_x)) \\ &- \psi_w \, \delta(\rho_w q_w) - \psi_n \, \delta(\rho_n q_n) \quad = \delta g. \end{aligned} \tag{74}$$

Further use of integration by parts and the chain rule produces the following form of the volume integrand where only variations of p and S appear:

$$\begin{aligned} &- (\psi_w)_t \left[(\rho_w' \phi + \rho_w \phi') S \delta p \quad + \rho_w \phi \delta S \right] \\ &- (\psi_n)_t \left[(\rho_n' \phi + \rho_n \phi')(1-S) \delta p \quad - \rho_n \phi \delta S \right] \\ &+ (\psi_w)_x \left[\rho_w' K \lambda_w p_x \delta p \quad + \rho_w K \lambda_w' p_x \delta S \right] \\ &+ (\psi_n)_x \left[(\rho_n' K \lambda_n)(p_x + \gamma S_x) \delta p \right] \\ &+ (\psi_n)_x \left[(\rho_n K \lambda_n')(p_x + \gamma S_x) \delta S \right] \\ &+ (\psi_n)_x \left[\rho_n K \lambda_n \gamma' S_x \delta S \right] \\ &- \psi_w \left[(\rho_w' q_w + \rho_w q_{w_p}) \delta p \quad + \rho_w q_{w_S} \delta S \right] \\ &- \psi_n \left[(\rho_n' q_n + \rho_n q_{n_p}) \delta p \quad + \rho_n q_{n_S} \delta S \right] \\ &- \left[\rho_w K \lambda_w (\psi_w)_x \right]_x \delta p \\ &- \left[\rho_n K \lambda_n (\psi_n)_x \right]_x \delta p \quad - \left[\rho_n K \lambda_n \gamma (\psi_n)_x \right]_x \delta S \\ &= g_p \delta p + g_S \delta S, \end{aligned} \tag{75}$$

where $q_{w_p} = \frac{\partial q_w}{\partial p}, q_{w_S} = \frac{\partial q_w}{\partial S}, q_{n_p} = \frac{\partial q_n}{\partial p}, q_{n_S} = \frac{\partial q_n}{\partial S}, g_p = \frac{\partial g}{\partial p}$ and $g_S = \frac{\partial g}{\partial S}$.

Grouping together terms that multiply δp and noting that Eq. (75) holds for any δp, yields the first adjoint equation, given in Eq. (76). Repeating the process for terms multiplying δS yields the second adjoint equa-

tion, given in Eq. (77).

$$
\begin{aligned}
&-(\psi_w)_t \cdot (\rho_w'\phi + \rho_w\phi')S \\
&-(\psi_n)_t \cdot (\rho_n'\phi + \rho_n\phi')(1-S) \\
&+(\psi_w)_x \cdot (\rho_w' K\lambda_w p_x) \\
&+(\psi_n)_x \cdot [(\rho_n' K\lambda_n)(p_x + \gamma S_x)] \\
&-[\rho_w K\lambda_w(\psi_w)_x]_x - [\rho_n K\lambda_n(\psi_n)_x]_x \\
&-\psi_w \cdot (\rho_w' q_w + \rho_w q_{w_p}) - \psi_n \cdot (\rho_n' q_n + \rho_n q_{n_p}) = g_p
\end{aligned} \tag{76}
$$

$$
\begin{aligned}
&-(\psi_w)_t \cdot (\rho_w\phi) \\
&-(\psi_n)_t \cdot (-\rho_n\phi) \\
&+(\psi_w)_x \cdot (\rho_w K\lambda_w' p_x) \\
&+(\psi_n)_x \cdot [(\rho_n K\lambda_n')(p_x + \gamma S_x) + \rho_n K\lambda_n\gamma' S_x] \\
&-[\rho_n K\lambda_n\gamma(\psi_n)_x]_x \\
&-\psi_w \cdot (\rho_w q_{w_S}) - \psi_n \cdot (\rho_n q_{n_S}) \qquad = g_S
\end{aligned} \tag{77}
$$

Next, the boundary conditions of the adjoint problem are derived by collecting the boundary integral terms from Eq. (72), and accounting for the integration by parts that led to Eq. (76) and (77). Specifically, the boundary integrals at $t = T$ are:

$$
\begin{aligned}
&\int_0^L [\psi_w(x,T)(\rho_w'\phi + \rho_w\phi')S]\,\delta p\; dx \\
&+\int_0^L [\psi_n(x,T)(\rho_n'\phi + \rho_n\phi')(1-S)]\,\delta p\; dx \\
&+\int_0^L [\psi_w(x,T)(\rho_w\phi) + \psi_n(x,T)(-\rho_n\phi)]\,\delta S\; dx = 0.
\end{aligned} \tag{78}
$$

Requiring Eq. (78) to hold for any δp and δS gives the following conditions on the adjoint variables:

$$
\begin{aligned}
&\psi_w(x,T)(\rho_w'\phi + \rho_w\phi')S \\
&+\psi_n(x,T)(\rho_n'\phi + \rho_n\phi')(1-S) = 0,
\end{aligned} \tag{79}
$$

and

$$
\rho_w\psi_w(x,T) - \rho_n\psi_n(x,T) = 0. \tag{80}
$$

Similarly, isolating the boundary integrals for the right boundary gives:

$$
\begin{aligned}
&\int_0^T [-\rho_w' K\lambda_w p_x\psi_w - \rho_n' K\lambda_n(p_x + \gamma S_x)\psi_n]\,\delta p \\
&+\int_0^T [\rho_w K\lambda_w(\psi_w)_x + \rho_n K\lambda_n(\psi_n)_x]\,\delta p \\
&+\int_0^T [-\rho_w K\lambda_w' p_x\psi_w]\,\delta S \\
&+\int_0^T [-(\rho_n K\lambda_n'(p_x + \gamma S_x) + \rho_n K\lambda_n\gamma' S_x)\psi_n]\,\delta S \\
&+\int_0^T [\rho_n K\lambda_n\gamma(\psi_n)_x]\,\delta S \\
&+\int_0^T [-\rho_w K\lambda_w\psi_w - \rho_n K\lambda_n\psi_n]\,\delta p_x \\
&+\int_0^T [-\rho_n K\lambda_n\gamma\psi_n]\,\delta S_x = 0.
\end{aligned} \tag{81}
$$

Inspecting the integrands in Eq. (81), and accounting for the nature of the imposed primal boundary conditions yields the adjoint boundary conditions at the right boundary. For example, if the primal problem imposes Dirichlet boundary conditions for pressure and saturation at the right boundary, then $\delta p(L,t) = \delta S(L,t) = 0$, and therefore the adjoint solutions would only need to satisfy the conditions corresponding to the δp_x and δS_x terms. Specifically:

$$
\rho_w K\lambda_w\psi_w(L,t) + \rho_n K\lambda_n\psi_n(L,t) = 0, \tag{82}
$$

$$
\rho_n K\lambda_n\gamma\psi_n(L,t) = 0. \tag{83}
$$

Assuming $\gamma \neq 0$, the two conditions above reduce to $\psi_w(L,t) = \psi_n(L,t) = 0$. Isolating the boundary integrals for the left boundary produces an equation similar to Eq. (81), from which the adjoint boundary conditions can be determined in an analogous manner to the right boundary. As before, the primal initial condition eliminates the need for an adjoint boundary condition at $t = 0$.

4.2 Relationship with Buckley-Leverett

It is possible to reduce the two-phase flow equations presented in Eq. (66) and (67) to the Buckley-Leverett equation given in Eq. (41) by assuming incompressibility (i.e. $\rho_w' = \rho_n' = \phi' = 0$), zero capillary pressure (i.e. $\gamma = 0$), and the absence of source terms ($q_w = q_n = 0$). Under these assumptions, the primal equations in Eq. (66) and (67) reduce to:

$$
\phi S_t - (K\lambda_w p_x)_x = 0, \tag{84}
$$

$$
-\phi S_t - (K\lambda_n p_x)_x = 0. \tag{85}
$$

Taking the sum of Eq. (84) and (85) produces an elliptic pressure equation:

$$-\left(K(\lambda_w+\lambda_n)p_x\right)_x = 0. \tag{86}$$

The Buckley-Leverett equation is a combination of the wetting-phase saturation equation (Eq. (84)) and the pressure equation (Eq. (86)). Integrating Eq. (86) in space shows that $-K(\lambda_w+\lambda_n)p_x$ is equal to a constant (namely, the total velocity u_T), thereby allowing the spatial flux in Eq. (84) to be written as:

$$-K\lambda_w p_x = u_T \frac{\lambda_w}{\lambda_w+\lambda_n} = u_T f_w(S), \tag{87}$$

where the last equality uses the definition of the wetting phase fractional flow function, $f_w(S) = \frac{\lambda_w}{\lambda_w+\lambda_n}$. Using Eq. (87) in Eq. (84) yields the Buckley-Leverett equation given in Eq. (41).

Eq. (84) and (86) are written in the space-time formulation as:

$$\nabla \cdot \vec{\hat{\mathbf{F}}}(\hat{\mathbf{u}}, \nabla\hat{\mathbf{u}}) = 0, \tag{88}$$

where $\hat{\mathbf{u}} = (p, S)^T$, and

$$\vec{\hat{\mathbf{F}}} = \begin{pmatrix} \vec{\hat{F}}_{BL} \\ \vec{\hat{F}}_p \end{pmatrix} = \left[\begin{pmatrix} -K\lambda_w p_x \\ -K(\lambda_w+\lambda_n)p_x \end{pmatrix}, \begin{pmatrix} \phi S \\ 0 \end{pmatrix} \right]. \tag{89}$$

As before, the adjoint problem for this new, but equivalent, set of primal equations is obtained by equating the linearized weak form to the linearized output:

$$\begin{aligned} &\int_\Omega \psi_{BL} \left(\nabla \cdot \delta\vec{\hat{F}}_{BL} \right) d\Omega \\ &+ \int_\Omega \psi_p \left(\nabla \cdot \delta\vec{\hat{F}}_p \right) d\Omega = \int_\Omega \delta g \; d\Omega, \end{aligned} \tag{90}$$

where the new adjoint vector $\hat{\boldsymbol{\psi}} = [\psi_{BL}, \psi_p]^T$ contains the adjoint solutions for the Buckley-Leverett and pressure equations respectively.

The relationship between $\hat{\boldsymbol{\psi}}$ and $\boldsymbol{\psi}$ is obtained by via the analysis presented in Appendix D, which derives a simple relationship between the adjoint solutions of two equivalent sets of primal equations that are linear combinations of each other. Following the definitions given in Appendix D, the transformation matrix $\mathbf{H}$ from the wetting-nonwetting primal equations to the Buckley-Leverett-pressure primal equations is:

$$\mathbf{H} = \begin{pmatrix} \frac{1}{\rho_w} & 0 \\ \frac{1}{\rho_w} & \frac{1}{\rho_n} \end{pmatrix}. \tag{91}$$

Eq. (144) states that $\hat{\boldsymbol{\psi}} = \mathbf{H}^{-T}\boldsymbol{\psi}$, which when applied to this particular problem, gives:

$$\begin{pmatrix} \psi_{BL} \\ \psi_p \end{pmatrix} = \begin{pmatrix} \rho_w\psi_w - \rho_n\psi_n \\ \rho_n\psi_n \end{pmatrix}. \tag{92}$$

The ability to derive analytical solutions for ψ_{BL}, as described in Appendix C, makes the above relationship useful for verifying numerical adjoint solutions of the two-phase flow equations, which do not have analytical solutions in general.

4.3 Numerical results

The space-time adaptive DG finite element method described in [22] is used to compute the adjoint solutions of a two-phase flow problem that is consistent with the Buckley-Leverett problem defined in Eq. (41) - (43). This requires setting Dirichlet BCs for saturation S along the $t = 0$, $x = 0$ and $x = L$ boundaries. The pressure p requires a Neumann BC at the $x = 0$ boundary, and Dirichlet BCs at the $t = 0$ and $x = L$ boundaries. The pressure gradient used for the Neumann BC is calculated from Eq. (87), to be consistent with the Dirichlet saturation condition given by Eq. (43) on the $x = 0$ boundary. No boundary conditions are imposed at the $t = T$ boundary, where all fluxes are evaluated from the states in the interior of the domain. The problem is incompressible and contains no source terms. However, a small amount of capillary pressure ($\gamma = 0.1$) is required to stabilize oscillations that occur at the shock due to the Gibbs' phenomenon. Although this is a slight deviation from the Buckley-Leverett problem, which assumes zero capillary effects, it has no discernible impact on the numerical solutions.

Figures 11 and 12 show contour plots of the two-phase flow adjoint solutions, ψ_w and ψ_n respectively, obtained using a second-order space-time DG finite element method with approximately 750,000 degrees of freedom per state variable. Figure 13 shows a plot of ψ_{BL}, computed using ψ_w and ψ_n according to the first equation in Eq. (92). Visually comparing Figure 13 with Figure 8 demonstrates that ψ_{BL} agrees well with the adjoint solution of the Buckley-Leverett equation. However, in order to make a more formal comparison, profiles of ψ_{BL} at different times are compared with the analytical Buckley-Leverett adjoint derived in Section 3.2, as shown in Figure 14. The near-perfect agreement between the two solutions except in the vicinity of the shocks provides a satisfactory numerical confirmation of Eq. (92).

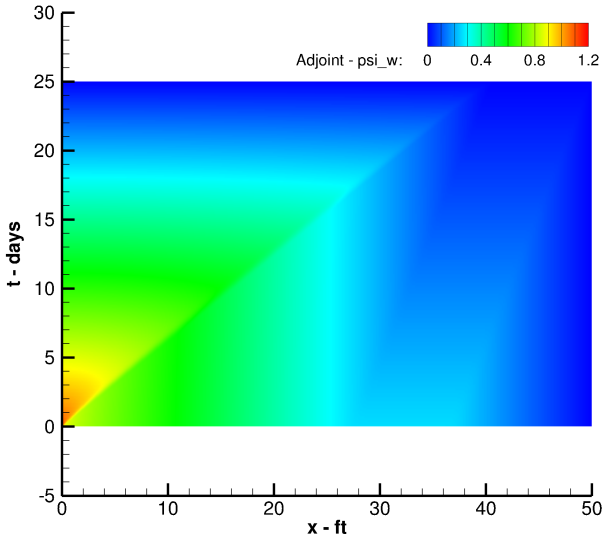

Fig. 11 Numerical adjoint solution ψ_w for output J from a second-order space-time DG method with 750,000 DOF per state variable.

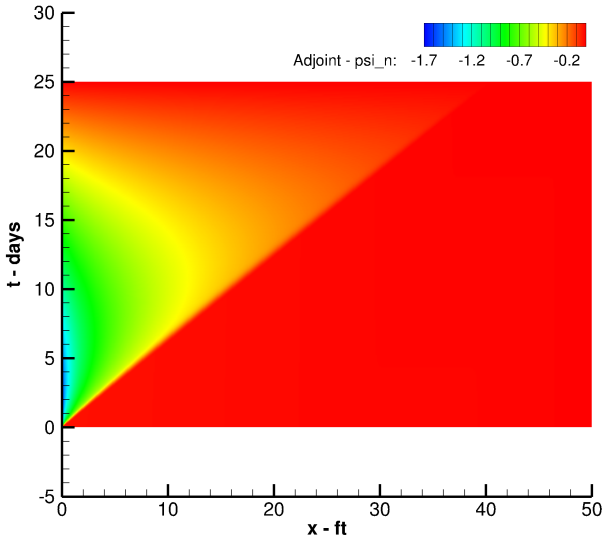

Fig. 12 Numerical adjoint solution ψ_n for output J from a second-order space-time DG method with 750,000 DOF per state variable.

5 Conclusions

This paper presents a derivation of the adjoint equation and boundary conditions for a scalar conservation law containing a shock, for two different output functionals: one involving a spatial integral and the other involving a space-time integral of solution dependent quantities. The results are specialized to the Buckley-Leverett problem, where attention to the combined rarefaction-shock wave behavior of the equations is essential to produce the correct analytical solution. In contrast to the behavior of equations with convex flux functions, such as the Burgers' equation, where the adjoint is continuous across a shock, the Buckley-Leverett equation is found to admit a discontinuous jump in adjoint value across a shock.

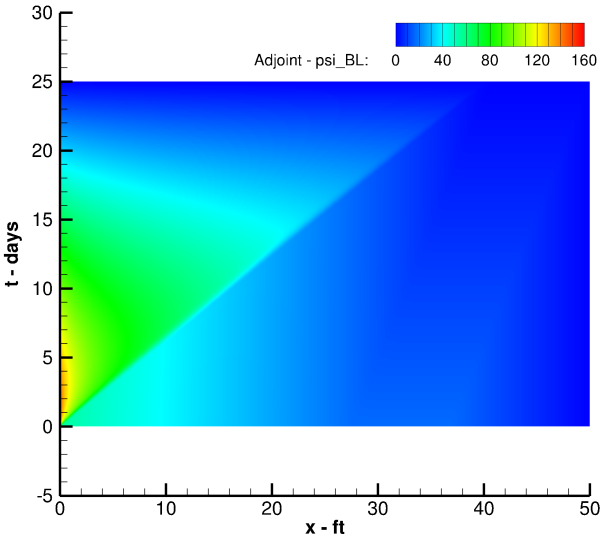

Fig. 13 Space-time contour plot of $\psi_{BL} = \rho_w \psi_w - \rho_n \psi_n$, computed from the numerical adjoint solutions.

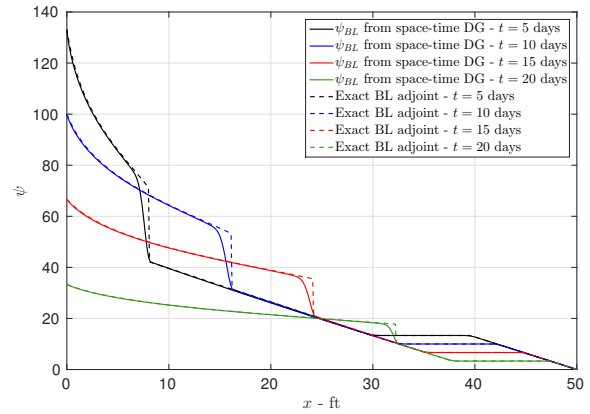

Fig. 14 Comparison of ψ_{BL} with the exact Buckley-Leverett adjoint at different times.

This work also presents the adjoint equations for the compressible two-phase flow equations in mass conservation form, and gives the relationship between the adjoint solutions of the two-phase flow and Buckley-Leverett problems, under appropriate assumptions. All space-time DG numerical results presented in this work are observed to be in good agreement with the derived analytical solutions.

The derivation of adjoint equations and boundary conditions for multi-dimensional, multi-phase flow problems is viewed as a tedious but straight-forward extension of the two-phase flow analysis presented in this paper. However, it is highly unlikely that closed-form analytic adjoint solutions exist for such complex problems, and therefore discrete approaches are necessary.

A Linearization of weighted residual

In order to simplify Eq. (16) further, consider the expression inside the brackets in the last integral of Eq. (16). Expanding out all components of space-time fluxes and normal vectors, and rewriting the expression in terms of 1D jump operators, yields:

$$\xi = \left[\!\!\left[\frac{\partial \vec{F}}{\partial x}\delta x_s\right]\!\!\right] + \left(\vec{F}^{+} - \vec{F}^{-}\right)\cdot \delta\vec{n}^{+} \tag{93}$$

$$= \left[\!\!\left[\left(\frac{\partial F_x}{\partial x}n_x + \frac{\partial F_t}{\partial x}n_t\right)\delta x_s\right]\!\!\right] + [\![F_x]\!]\,\delta n_x^{+} + [\![F_t]\!]\,\delta n_t^{+}, \tag{94}$$

where δn_x^{+} and δn_t^{+} are the spatial and temporal components of the perturbed unit normal vector of Γ_s. Since δx_s is unique for both sides of the shock, it is moved out of the jump operator, and the $\frac{\partial F_x}{\partial x}$ term is replaced with $-\frac{\partial F_t}{\partial t}$ using the space-time primal equation in Eq. (5), giving:

$$\xi = \left(\left[\!\!\left[\frac{\partial F_x}{\partial x}\right]\!\!\right] + \left[\!\!\left[\frac{\partial F_t}{\partial x}\right]\!\!\right]\frac{n_t^{+}}{n_x^{+}}\right) n_x^{+}\delta x_s + [\![F_x]\!]\,\delta n_x^{+} + [\![F_t]\!]\,\delta n_t^{+} \tag{95}$$

$$= \left(\left[\!\!\left[-\frac{\partial F_t}{\partial t} - \dot{x}_s\frac{\partial F_t}{\partial x}\right]\!\!\right]\right) n_x^{+}\delta x_s + [\![F_x]\!]\,\delta n_x^{+} + [\![F_t]\!]\,\delta n_t^{+}. \tag{96}$$

Following the approach used in [13] and using the definition $\frac{d(\cdot)}{dt} = \frac{\partial(\cdot)}{\partial t} + \dot{x}_s\frac{\partial(\cdot)}{\partial x}$, yields:

$$\frac{d\,[\![F_t]\!]}{dt} = \left[\!\!\left[\frac{\partial F_t}{\partial t} + \dot{x}_s\frac{\partial F_t}{\partial x}\right]\!\!\right], \tag{97}$$

and therefore:

$$\xi = -\frac{d\,[\![F_t]\!]}{dt}n_x^{+}\delta x_s + [\![F_x]\!]\,\delta n_x^{+} + [\![F_t]\!]\,\delta n_t^{+}. \tag{98}$$

Expanding the space-time jump condition in Eq. (7) gives:

$$[\![F_x]\!] = -\,[\![F_t]\!]\,\frac{n_t^{+}}{n_x^{+}}, \tag{99}$$

which is substituted in Eq. (98) to obtain:

$$\xi = -\frac{d\,[\![F_t]\!]}{dt}n_x^{+}\delta x_s - [\![F_t]\!]\left(\frac{n_t^{+}\delta n_x^{+}}{n_x^{+}} - \delta n_t^{+}\right). \tag{100}$$

The final step requires a relationship between δx_s and the components of the perturbed unit normal vector $\vec{n}^{+}$. This is derived by linearizing the ratio of n_t^{+}/n_x^{+} as defined in Eq. (10):

$$\dot{x}_s = -\frac{n_t^{+}}{n_x^{+}} \tag{101}$$

$$\dot{x}_s + \delta\dot{x}_s = -\frac{n_t^{+} + \delta n_t^{+}}{n_x^{+} + \delta n_x^{+}}. \tag{102}$$

Eq. (102) is simplified further using a Taylor series expansion of the right-hand side and retaining the linear terms as follows:

$$\dot{x}_s + \delta\dot{x}_s = -\left(n_t^{+} + \delta n_t^{+}\right)\left(\frac{1}{n_x^{+}} - \frac{\delta n_x^{+}}{n_x^{2^{+}}} + \mathcal{O}(\delta n_x^{2^{+}})\right) \tag{103}$$

$$\delta\dot{x}_s = \frac{n_t^{+}\delta n_x^{+}}{n_x^{2^{+}}} - \frac{\delta n_t^{+}}{n_x^{+}}. \tag{104}$$

Noting that the right-hand side of Eq. (104) appears inside the brackets of the last term in Eq. (100), the expression for ξ is finally given by:

$$\xi = -\frac{d\,[\![F_t]\!]}{dt}n_x^{+}\delta x_s - [\![F_t]\!]\,\delta\dot{x}_s n_x^{+} \tag{105}$$

$$= -\frac{d}{dt}\left([\![F_t]\!]\,\delta x_s\right)n_x^{+} \tag{106}$$

$$= -\frac{d}{dt}\left((F_t^{+} - F_t^{-})\delta x_s\right)n_x^{+}. \tag{107}$$

B Output sensitivities via adjoint solutions

This section outlines how solutions to the continuous adjoint problem can be used to compute the sensitivities of an output functional to parameters in the model. Assume that the weak form residual equation which needs to be satisfied by the primal solution $u(x,t,\alpha)$ is given by:

$$R(u, w, \alpha) = 0, \tag{108}$$

where $w(x,t)$ is an admissible test function and α is a model parameter. The linearized form of the above equation is obtained by considering infinitesimal perturbations of α as follows:

$$\begin{aligned} R(u+\delta u, w, \alpha+\delta\alpha) &= 0, \\ \delta R(\delta u, w, \delta\alpha) &= 0. \end{aligned} \tag{109}$$

Furthermore, the δR constraint in Eq. (109) can be expanded as:

$$\delta R(\delta u, w, 0) + \delta R(0, w, \delta\alpha) = 0. \tag{110}$$

For a given generic output function $J(u,\alpha)$, the adjoint solution $\psi(x,t)$ satisfies the following equation for all δu:

$$\delta R(\delta u, \psi, 0) = \delta J(\delta u, 0). \tag{111}$$

The total perturbation in the output is given by $\delta J(\delta u, \delta\alpha)$, which can be decomposed and re-written using Eq. (111) and (110) as:

$$\begin{aligned} \delta J(\delta u, \delta\alpha) &= \delta J(\delta u, 0) + \delta J(0, \delta\alpha) \\ &= -\delta R(0, \psi, \delta\alpha) + \delta J(0, \delta\alpha) \end{aligned} \tag{112}$$

It is worth noting that the absence of δu in the right-hand side of Eq. (112) allows the output perturbation to be evaluated directly from $\delta\alpha$ without first calculating δu. Therefore, this adjoint-based sensitivity method is more efficient than the direct method when multiple sensitivity evaluations are required.

C Analytic adjoint solutions for Buckley-Leverett

This section presents a derivation of analytical solutions for the Buckley-Leverett adjoint problems considered in Sections 3.1 and 3.2, using the method of characteristics.

The adjoint PDEs given in Eq. (51) and (60) are written in a general form as follows:

$$\frac{\partial\psi}{\partial t} + a\frac{\partial\psi}{\partial x} = q, \tag{113}$$

where $a(S_w(x,t)) = \frac{u_T}{\phi}\frac{\partial f_w}{\partial S_w}$, and $q(S_w(x,t))$ is the source-term of each adjoint equation. The first-order linear PDE in Eq. (113) is transformed into an ODE along the characteristic curve $(x_c(\eta), t_c(\eta))$.

$$\frac{d\psi}{d\eta} = \frac{\partial\psi}{\partial x_c}\frac{dx_c}{d\eta} + \frac{\partial\psi}{\partial t_c}\frac{dt_c}{d\eta} \tag{114}$$

Assuming that $\frac{dx_c}{d\eta} = a$ and $\frac{dt_c}{d\eta} = 1$ simplifies Eq. (114) to:

$$\frac{d\psi}{d\eta} = a\frac{\partial\psi}{\partial x_c} + \frac{\partial\psi}{\partial t_c} = q. \tag{115}$$

The characteristic paths of the primal and dual problems for Buckley-Leverett are identical, and the primal solution $S_w(x,t)$ remains constant along each characteristic path. This allows for a straight-forward integration of the ODEs assumed above, $\frac{dx_c}{d\eta} = a$ and $\frac{dt_c}{d\eta} = 1$, producing the following linear expressions for the characteristic path:

$$x_c(\eta) = a\eta + x^*, \tag{116}$$
$$t_c(\eta) = \eta + t^*, \tag{117}$$

where (x^*, t^*) denotes the space-time location of where the adjoint value is desired. If the characteristic line through the point of interest (x^*, t^*) terminates at the top boundary, then Eq. (115) is integrated along that characteristic from $\eta = \eta_0 = 0$ to $\eta = \eta_T = (T - t^*)$, to obtain:

$$\psi(\eta_T) - \psi(\eta_0) = \int_{\eta_0}^{\eta_T} q\ d\eta \tag{118}$$

$$\psi(x_T, T) - \psi(x^*, t^*) = \int_0^{T-t^*} q\ dt \tag{119}$$

$$\psi(x^*, t^*) = \psi(x_T, T) - \int_0^{T-t^*} q\ dt, \tag{120}$$

where x_T denotes the x-location of the characteristic at $t = T$, which is given by:

$$x_T = x^* + a(S_w(x^*, t^*)) \cdot (T - t^*). \tag{121}$$

Since the adjoint source term $q(S_w(x,t))$ is also constant along a given characteristic, the integral in Eq. (120) evaluates to:

$$\boxed{\psi(x^*, t^*) = \psi(x_T, T) - q(S_w(x^*, t^*)) \cdot (T - t^*).} \tag{122}$$

If $x_T > L$, then the characteristic through (x^*, t^*) exits the domain via the right boundary, and therefore a slightly modified version of Eq. (122) is required to obtain $\psi(x^*, t^*)$:

$$\boxed{\psi(x^*, t^*) = \psi(L, t_B) - q(S_w(x^*, t^*)) \cdot (t_B - t^*).} \tag{123}$$

where t_B is the time at which the characteristic reaches the right boundary, and $\psi(L, t_B)$ is specified by the adjoint boundary condition.

Similarly, if the characteristic line through the point (x^*, t^*) terminates at the shock interface, then integrating Eq. (115) along that characteristic from $\eta = \eta_0 = 0$ to $\eta = \eta_s = (t_s - t^*)$ yields:

$$\psi(\eta_s) - \psi(\eta_0) = \int_{\eta_0}^{\eta_s} q\ d\eta \tag{124}$$

$$\psi(x^*, t^*) = \psi(x_s^-(t_s), t_s) - q(S_w(x^*, t^*)) \cdot (t_s - t^*), \tag{125}$$

where t_s denotes the time at which the characteristic line intersects the shock. In this case, t_s is calculated by solving the following equation:

$$x_s(t_s) = x^* + a(S_w(x^*, t^*)) \cdot (t_s - t^*), \tag{126}$$

where $x_s(t_s)$ is the shock location at time t_s. Recalling that the shock speed $\dot{x}_s$ is constant and that $x_s(0) = 0$, gives an explicit expression for t_s:

$$t_s = \frac{x^* - a \cdot t^*}{\dot{x}_s - a}. \tag{127}$$

The result of Eq. (58) and the value of t_s from above simplifies Eq. (125) to:

$$\boxed{\psi(x^*, t^*) = \psi_s(t_s) - q(S_w(x^*, t^*)) \cdot (t_s - t^*),} \tag{128}$$

where $\psi_s(t_s)$ is known from Eq. (55) or Eq. (64), depending on the output functional used.

D Adjoint relationships between equivalent sets of PDEs

Consider the following linearized primal problem:

$$Lu = f, \qquad \text{in } \Omega, \tag{129}$$
$$Bu = e, \qquad \text{on } \Gamma, \tag{130}$$

where $u \in \mathbb{R}^n$ is the primal solution vector, $L : \mathbb{R}^n \to \mathbb{R}^n$ is a linear differential operator in the domain $\Omega \in \mathbb{R}^d$, and $B : \mathbb{R}^n \to \mathbb{R}^n$ represents the primal boundary condition operator on $\Gamma \in \mathbb{R}^{d-1}$.

The following notation for volume and boundary inner products,

$$(u, v) = \int_\Omega u^T v\ d\Omega, \tag{131}$$
$$\langle u, v\rangle = \int_\Gamma u^T v\ d\Gamma, \tag{132}$$

allows the output of interest to be written as:

$$J = (g, u) + \langle g_B, u\rangle. \tag{133}$$

The duality condition produces the following relationship:

$$(g, u) + \langle g_B, u\rangle = (\psi, f) + \langle C^*\psi, e\rangle, \tag{134}$$

which is used to derive the corresponding dual problem:

$$L^*\psi = g, \qquad \text{in } \Omega, \tag{135}$$
$$B^*C^*\psi = g_B, \qquad \text{on } \Gamma, \tag{136}$$

where the adjoint operators L^*, B^* and C^* are derived using integration by parts, as described for the porous media model equations in the main body of the paper.

Next, consider an equivalent set of primal equations defined by the transformation matrices $M \in \mathbb{R}^{n\times n}$ and $H \in \mathbb{R}^{n\times n}$:

$$\hat{u} = Mu, \tag{137}$$
$$\hat{f} = Hf. \tag{138}$$

Rewriting the primal problem in terms of these new quantities yields:

$$\hat{L}\hat{u} = \hat{f}, \qquad \text{in } \Omega, \tag{139}$$

$$\hat{B}\hat{u} = e, \qquad \text{on } \Gamma, \tag{140}$$

where $\hat{L} = HLM^{-1}$ and $\hat{B} = BM^{-1}$. Similarly, rewriting the output functional gives $J = (\hat{g}, \hat{u}) + \langle \hat{g}_B, \hat{u} \rangle$, where $\hat{g} = M^{-T} g$ and $\hat{g}_B = M^{-T} g_B$.

The duality condition for the transformed problems is manipulated as follows:

$$(\hat{g}, \hat{u}) + \langle \hat{g}_B, \hat{u} \rangle = (\hat{\psi}, \hat{f}) + \langle \hat{C}^* \hat{\psi}, e \rangle \tag{141}$$

$$(M^{-T} g, Mu) + \langle M^{-T} g_B, Mu \rangle = (\hat{\psi}, Hf) + \langle \hat{C}^* \hat{\psi}, e \rangle \tag{142}$$

$$(g, u) + \langle g_B, u \rangle = (H^T \hat{\psi}, f) + \langle \hat{C}^* \hat{\psi}, e \rangle \tag{143}$$

Comparing the volume integrals of Eq. (134) and Eq. (143) gives the relationship between the adjoint variables of the original primal problem and those of the transformed primal problem:

$$\hat{\psi} = H^{-T} \psi. \tag{144}$$

Further, comparing the boundary integrals yields $\hat{C}^* = C^* H^T$. Note that the adjoint variable transformation given in Eq. (144) is independent of the solution variable transformation matrix M.

Acknowledgements The authors wish to thank Dr. Eric Dow for reviewing this paper.

References

1. Alauzet, F., Pironneau, O.: Continuous and discrete adjoints to the Euler equations for fluids. International Journal for Numerical Methods in Fluids **70**(2), 135–157 (2012)
2. Awotunde, A.A., Horne, R.: An Improved Adjoint-Sensitivity Computation for Multiphase Flow Using Wavelets. Society of Petroleum Engineers (2012)
3. Aziz, K., Settari, A.: Petroleum Reservoir Simulation. Elsevier (1979)
4. Barth, T.J., Larson, M.G.: A posteriori error estimates for higher order Godunov finite volume methods on unstructured meshes. In: R. Herban, D. Kröner (eds.) Finite Volumes for Complex Applications III. Hermes Penton, London (2002)
5. Becker, R., Rannacher, R.: A feed-back approach to error control in finite element methods: Basic analysis and examples. East-West Journal of Numerical Mathematics **4**, 237–264 (1996)
6. Becker, R., Rannacher, R.: An optimal control approach to a posteriori error estimation in finite element methods. In: A. Iserles (ed.) Acta Numerica. Cambridge University Press (2001)
7. Chavent, G., Dupuy, M., Lemmonier, P.: History Matching by Use of Optimal Theory. Society of Petroleum Engineers **15**(1), 74–86 (1975)
8. Chen, W., Gavalas, G., Seinfeld, J., Wasserman, M.: A New Algorithm for Automatic History Matching. Society of Petroleum Engineers **14**(6), 593–608 (1974)
9. Eydinov, D., Aanonsen, S.I., Haukås, J., Aavatsmark, I.: A method for automatic history matching of a compositional reservoir simulator with multipoint flux approximation. Computational Geosciences **12**(2), 209–225 (2008)
10. Fidkowski, K., Darmofal, D.: Review of output-based error estimation and mesh adaptation in computational fluid dynamics. AIAA Journal **49**(4), 673–694 (2011)
11. Giles, M.: Discrete adjoint approximations with shocks. In: T. Hou, E. Tadmor (eds.) Hyperbolic Problems: Theory, Numerics, Applications. Springer-Verlag (2003)
12. Giles, M., Pierce, N.: Adjoint error correction for integral outputs. In: T. Barth, M. Griebel, D.E. Keyes, R.M. Nieminen, D. Roose, T. Schlick (eds.) Lecture Notes in Computational Science and Engineering: Error Estimation and Adaptive Discretization Methods in Computational Fluid Dynamics, vol. 25. Springer, Berlin (2002)
13. Giles, M., Ulbrich, S.: Convergence of linearized and adjoint approximations for discontinuous solutions of conservation laws. part 1: Linearized approximations and linearized output functionals **48**(3), 882–904 (2010)
14. Giles, M.B., Pierce, N.A.: Adjoint equations in CFD: duality, boundary conditions, and solution behaviour. AIAA 97-1850 (1997)
15. Giles, M.B., Pierce, N.A.: An introduction to the adjoint approach to design. Flow, Turbulence and Combustion **65**, 393–415 (2000). DOI 10.1023/A:1011430410075
16. Giles, M.B., Pierce, N.A.: Analytic adjoint solutions for the quasi-one dimensional Euler equations. J. Fluid Mech. pp. 327–345 (2001)
17. Giles, M.B., Süli, E.: Adjoint methods for PDEs: a posteriori error analysis and postprocessing by duality. In: Acta Numerica, vol. 11, pp. 145–236 (2002)
18. González-Rodríguez, P., Kindelan, M., Moscoso, M., Dorn, O.: History matching problem in reservoir engineering using the propagation-backpropagation method. Inverse Problems **21**(2), 565 (2005)
19. Hartmann, R.: Adjoint consistency analysis of discontinuous Galerkin discretizations. SIAM Journal on Numerical Analysis **45**(6), 2671–2696 (2007)
20. Hartmann, R., Houston, P.: Error estimation and adaptive mesh refinement for aerodynamic flows. In: H. Deconinck (ed.) VKI LS 2010-01: 36$^{\text{th}}$ CFD/ADIGMA course on hp-adaptive and hp-multigrid methods, Oct. 26-30, 2009. Von Karman Institute for Fluid Dynamics, Rhode Saint Genèse, Belgium (2009)
21. Jayasinghe, S., Darmofal, D.L., Burgess, N.K., Galbraith, M.C., Allmaras, S.R.: A space-time adaptive method for reservoir flows: formulation and one-dimensional application. Computational Geosciences (2017)
22. Jayasinghe, Y.S.: A Space-time Adaptive Method for Flows in Oil Reservoirs. Master's thesis, Mass. Inst. of Tech., Department of Aeronautics and Astronautics (2015)
23. Kourounis, D., Durlofsky, L.J., Jansen, J.D., Aziz, K.: Adjoint formulation and constraint handling for gradient-based optimization of compositional reservoir flow. Computational Geosciences **18**(2), 117–137 (2014)
24. Li, R., Reynolds, A., Oliver, D.: History Matching of Three-Phase Flow Production Data. Society of Petroleum Engineers (2003)
25. Loseille, A., Dervieux, A., Alauzet, F.: Fully anisotropic goal-oriented mesh adaptation for 3d steady Euler equations. Journal of Computational Physics **229**, 2866–2897 (2010)
26. Oliver, D.S., Reynolds, A.C., Liu, N.: Inverse Theory for Petroleum Reservoir Characterization and History Matching (2008)

27. Venditti, D.A., Darmofal, D.L.: Grid adaptation for functional outputs: application to two-dimensional inviscid flows. Journal of Computational Physics **176**(1), 40–69 (2002)
28. Venditti, D.A., Darmofal, D.L.: Anisotropic grid adaptation for functional outputs: Application to two-dimensional viscous flows. Journal of Computational Physics **187**(1), 22–46 (2003)
29. Wasserman, M., Emanuel, A., Seinfeld, J.: Practical Applications of Optimal-Control Theory to History-Matching Multiphase Simulator Models. Society of Petroleum Engineers **15**(4), 347–355 (1975)
30. Wu, Z., Reynolds, A., Oliver, D.: Conditioning Geostatistical Models to Two-Phase Production Data. Society of Petroleum Engineers (1999)
31. Yano, M.: An optimization framework for adaptive higher-order discretizations of partial differential equations on anisotropic simplex meshes. PhD thesis, Massachusetts Institute of Technology, Department of Aeronautics and Astronautics (2012)